# Journal Name

## ARTICLE

# Photoinduced hydrogen evolution with new tetradentate cobalt(II) complexes based on the TPMA ligand.

Mirco Natali,*[a] Elena Badetti,[b] Elisa Deponti,[a] Marta Gamberoni,[a] Francesca A. Scaramuzzo,[b] Andrea Sartorel[b] and Cristiano Zonta*[b]

Hydrogen production from water splitting is nowadays recognized as a target, fundamental reaction for the production of clean fuels. Indeed, tremendous efforts have been devoted towards the research of suitable catalysts capable of performing this reaction. With respect to heterogeneous systems, molecular catalysts such as metal complexes are amenable to chemical functionalization in order to fine tune the catalytic properties. In this paper a new class of tris(2-pyridylmethyl)-amine (**TPMA**) cobalt(II) complexes (**CoL0-4**) has been synthesized and employed as hydrogen evolving catalysts under photochemical conditions taking advantage of $Ru(bpy)_3^{2+}$ (where bpy is 2,2'-bipyridyne) as the light-harvesting sensitizer and ascorbic acid as the sacrificial electron donor. Tuning of the photocatalytic activity has been attempted through the introduction of different substituents at the catalyst periphery rather than through a direct chemical modification of the chelating **TPMA** ligand. The results show that **CoL0-4** behave as competent hydrogen evolving catalysts (HECs), although the effects played by the different substituents on the catalysis are relatively modest. Possible reasons supporting the observed behavior as well as possible improvements of the aforementioned tuning approach are discussed.

## Introduction

Hydrogen production from water splitting represents one of the target processes for the production of clean fuels for a sustainable development. Moreover, the use of a renewable energy supply such as solar energy to drive this reaction would in principle allow the mankind to solve both the energetic and environmental problems of the current century.[1] To this purpose substantial efforts have been undertaken for the development of efficient proton reduction catalysts, both at the heterogeneous and homogeneous level, and to study their possible coupling with light.[2] Among the heterogeneous catalysts, platinum metal,[3] NiMoZn alloys,[4] and W or Mo sulfides[5] have proven to be efficient and stable materials for the hydrogen evolution reaction (HER) with the capability of being also easily incorporated into artificial devices.[6] As far as homogeneous molecular catalysts are concerned, particular attention has been mainly devoted to the study of noble-metal-free species, including (i) diiron hydrogenase mimics,[7] (ii) nickel compounds with diphosphine ligands,[8] and (iii)

macrocyclic cobalt complexes[9] with cobaloximes playing the major role.[10] More recently, polypyridine cobalt complexes have also emerged as active molecular catalysts for the HER in aqueous solutions, combining an efficient activity in light-activated experiments with a good stability under turnover conditions.[11]

Though being usually less stable than inorganic materials, molecular catalysts are, on the other hand, amenable to synthetic functionalization, e.g., by metal changing or ligand substitution, with the possibility of tuning the catalytic activity towards the optimization of the performances under both dark (electrocatalytic) and light-activated (photocatalytic) conditions.[11b,h,12] For instance, several works on cobalt-based molecular catalysts have targeted the functionalization of cobaloximes,[13] polypyridine,[14] or dithiolene cobalt complexes[15] with different groups, either electron withdrawing or electron donating ones, in order to finely adjust the reduction potential of the cobalt center and thus its catalytic ability. The functionalization of the β-position of a cobalt corrole with different halides was also recently exploited to optimize the catalytic performance under electrochemical conditions.[16] By adopting a different approach to the catalyst tuning, a carboxylic acid functional group was introduced at the periphery of a cobalt porphyrin hydrogen evolving catalyst resulting in a lower overpotential for the HER with respect to the unfunctionalized porphyrin thanks to the possibility of intramolecular proton-coupled electron-transfer.[17]

Herein, we investigate the photocatalytic hydrogen evolution ability of a new class of cobalt polypyridine complexes (**CoL0-4**)
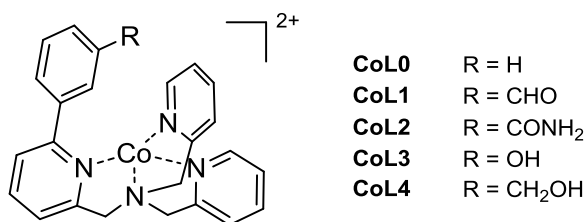
**Chart 1.** Isostructural molecular cobalt(II) catalysts studied in this work. In all cases the anion is perchlorate.



| | |
|---|---|
| **CoL0** | R = H |
| **CoL1** | R = CHO |
| **CoL2** | R = $CONH_2$ |
| **CoL3** | R = OH |
| **CoL4** | R = $CH_2OH$ |

based on variations of the tetradentate tris(2-pyridylmethyl)-amine (**TPMA**) ligand (Chart 1). In these systems, the appropriate introduction of different functional groups in *meta* position to a phenyl moiety in *alpha* to one pyridine ring is performed in order to influence the second sphere interactions of the catalytic center. The approach adopted herein should provide an additional way, alternative to the use of proton relays based on amine groups,[8] in order to tune and optimize the catalytic ability of molecular catalysts without affecting the electronic properties of the metal center.
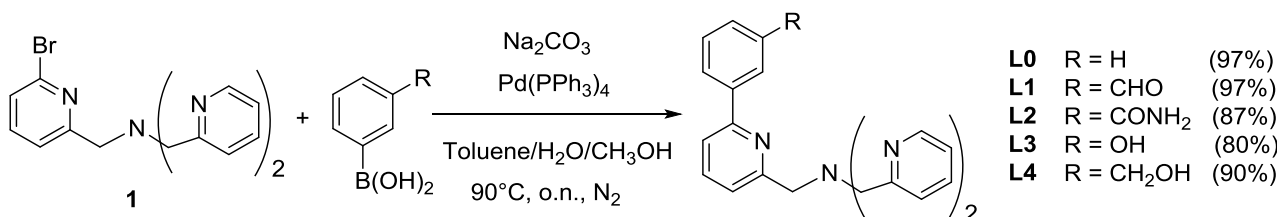
## Results and discussions

### Synthesis

The general procedures for the synthesis of the **TPMA** ligands and complexes **CoL0-4** are summarized in Schemes 1 and 2, respectively. We first synthesized the ligands **L0-4**, consisting of the **TPMA** core bearing different substituents on one of the three arms (Scheme 1). The method, already developed by us for the synthesis of **L0-1**,[18] consists in the formation of compound **1** via reductive amination of commercially available 6-bromo-2-pyridinecarboxaldehyde and di(2-picolyl)amine followed by a Suzuki coupling with the boronic acid of interest. In general, 4.9 mmol of ligand **1**, 7.3 mmol of the desired boronic acid, 12.2 mmol of $Na_2CO_3$ and 0.49 mmol of $Pd(PPh_3)_4$

are dissolved in 50 mL of degassed $H_2O$/toluene/$CH_3OH$ (1:1:0.5) under $N_2$ atmosphere. The mixture is stirred for 10 h at 90°C. After an acid/base work-up of the reaction mixture the final product is obtained in high yields. The syntheses have also been optimized for ligands **L2-4** on a gram scale without requiring modification of the protocol. The obtained products have been fully characterized by $^1$H-NMR, $^{13}$C-NMR, IR, ESI-MS, and elemental analysis (see ESI). The general procedure for the synthesis of Co(II) complexes **CoL0-4** (Scheme 2) involves the mixing of an equimolar amount of $Co(ClO_4)_2 \cdot 6H_2O$ to the corresponding ligands **L0-4** in acetonitrile. The solutions are left at room temperature for 30 minutes and the desired compounds are obtained as powders by precipitation with diethyl ether. These compounds have also been fully characterized by IR, ESI-MS, and elemental analysis (see ESI).
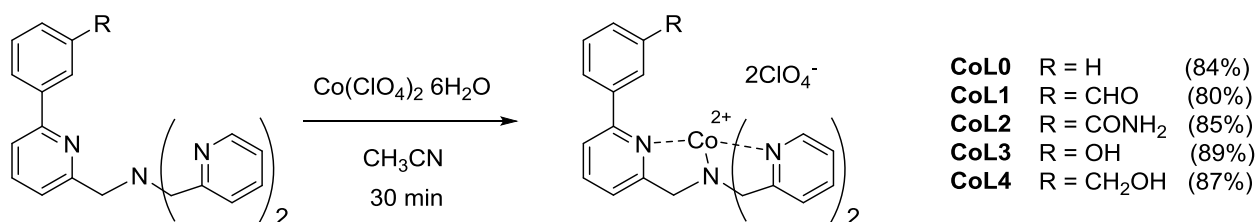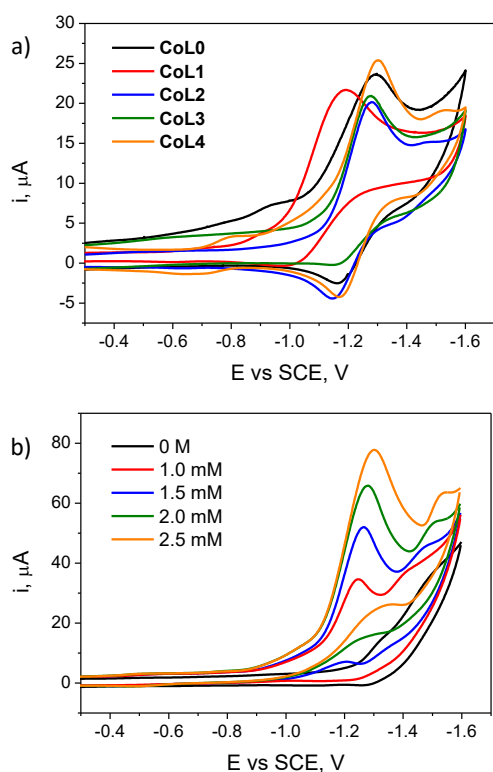
### Electrochemical characterization

In order to get information on the effective ability of the cobalt(II) complexes examined (**CoL0-4**) to act as hydrogen evolving catalysts (HECs) under photochemical conditions, electrochemical experiments were first performed. In nitrogen-purged acetonitrile (0.1 M $LiClO_4$) reversible processes can be detected at $E_{1/2}$ = −1.23 V vs. SCE for **CoL0**, at $E_{1/2}$ = −1.22 V vs. SCE for both **CoL2** and **CoL3**, and at $E_{1/2}$ = −1.24 V vs. SCE for **CoL4**, which can be attributed to Co(II)/Co(I) reductions (Figure 1a). In the case of **CoL1** the same process is slightly shifted towards more positive potentials and becomes less reversible with a peak potential of $E_{pc}$ = −1.19 V vs. SCE. The small differences (within ca 50 mV) in terms of reduction potential within the class of complexes is consistent with a weak electronic effect played by the different substituents on the cobalt center. When the solvent is changed from pure acetonitrile to a 50/50 acetonitrile/water mixture,‡ the Co(II)/Co(I) reduction process shifts by ca 100-200 mV towards more negative potentials and becomes

**Scheme 1.** General synthetic procedure for the synthesis of the ligands **L0-4**; reaction yields are reported in brackets.



| | | |
|---|---|---|
| **L0** | R = H | (97%) |
| **L1** | R = CHO | (97%) |
| **L2** | R = $CONH_2$ | (87%) |
| **L3** | R = OH | (80%) |
| **L4** | R = $CH_2OH$ | (90%) |

**Scheme 2.** General synthetic procedure for the synthesis of **CoL0-4**; reaction yields are reported in brackets.



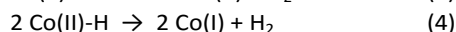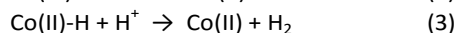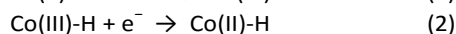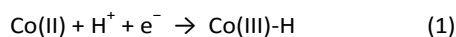| | | |
|---|---|---|
| **CoL0** | R = H | (84%) |
| **CoL1** | R = CHO | (80%) |
| **CoL2** | R = $CONH_2$ | (85%) |
| **CoL3** | R = OH | (89%) |
| **CoL4** | R = $CH_2OH$ | (87%) |

**ARTICLE**



**Figure 1.** (a) Cyclic voltammetry (CV) of **CoL0-4** in nitrogen-purged acetonitrile (0.1 M LiClO₄); (b) cyclic voltammetry (CV) of 1 mM **CoL0** in nitrogen-purged 50/50 acetonitrile/water (0.1 M LiClO₄) upon addition of 0-2.5 mM TFA. Experimental conditions: GC as working electrode, Pt as counter electrode, SCE as reference electrode, room temperature, scan rate *v* = 100 mV/s.

generally broad and irreversible (see Figure 1b for **CoL0** and Figure S1 for the remaining complexes **CoL1-4**). Under these conditions, water can indeed act as proton source on the electrogenerated Co(I) species, thus explaining the irreversibility of the process.§ More interestingly, in all cases the addition of trifluoroacetic acid (TFA) triggers the appearance of new waves near the Co(II)/Co(I) process which increase in intensity with increasing TFA concentration (Figure 1b for **CoL0** and Figure S1 for the remaining complexes **CoL1-4**) and can be ascribed to catalytic proton reduction by the cobalt complexes.[11] This attribution is further confirmed by the evolution of hydrogen upon bulk electrolysis at a constant potential of E = −1.20 V vs. SCE on a 1 mM **CoL3** solution in 50/50 acetonitrile/water (2.5 mM TFA, 0.1 M LiClO₄ as supporting electrolyte) using a carbon foil as the working electrode (see Experimental Section for additional details and Figure S2). Noteworthy, the ratio between the amount of hydrogen formed and the theoretical amount expected from the charge passed indicates a Faradaic Efficiency (FE) close to 90% (Figure S2c). The catalytic waves display an onset potential of ca −1.00 V vs. SCE, irrespective of the substituent present on the phenyl ring connected to the **TPMA** ligand. Importantly, these waves precede the Co(II)/Co(I) reduction steps, thus implying that catalytic hydrogen evolution by the **CoL0-4** complexes is triggered by an EC process, namely the

one-electron reduction of Co(II) to Co(I) followed by a chemical process such as protonation (eq 1), with formation of a key Co(III)-hydride intermediate.[19] Moreover, the onset of the catalytic waves falls at an appreciably constant potential as long as the TFA concentration is increased (i.e., the pH is decreased). This can be taken as an indication[19] that, under these experimental conditions, an additional reduction of the Co(III)-hydride (eq 2) is also required prior to hydrogen release. The resulting Co(II)-H species should then be capable of evolving hydrogen in either a heterolytic (protonation) or a homolytic (disproportionation) pathway (eq 3 or 4, respectively).[20]

$$Co(II) + H^+ + e^- \rightarrow Co(III)\text{-}H \qquad (1)$$
$$Co(III)\text{-}H + e^- \rightarrow Co(II)\text{-}H \qquad (2)$$
$$Co(II)\text{-}H + H^+ \rightarrow Co(II) + H_2 \qquad (3)$$
$$2\,Co(II)\text{-}H \rightarrow 2\,Co(I) + H_2 \qquad (4)$$

It can be observed that for all **CoL0-4** complexes the peak currents of the catalytic waves display an appreciably linear correlation with respect to the TFA concentration (Figure S3), indicating that catalysis follows a second-order with respect to the acid.[21,22] The linear dependence of the catalytic current vs. acid concentration together with the shape of the cyclic voltammograms (Figure 1b and Figure S1) thus suggest that, under these experimental conditions, catalysis is likely to fall under the "total catalysis" regime defined by Savéant[23] and is thus limited by the diffusion of the substrate into the reaction layer.§§ Under these kinetic conditions the extrapolation of mechanistic information as well as the relevant kinetic parameters from the catalytic peak current is not directly applicable.[24]

In order to attain a deeper mechanistic insight, taking **CoL0** as a reference for all complexes, it can be seen that, in the presence of an excess TFA proton source, the catalytic current is linearly dependent on the catalyst concentration (Figure S4), thus suggesting a first-order process with respect to the catalyst.[21,22] This latter behavior is in principle compatible with both a heterolytic mechanism (eq 1,2,3) and a homolytic pathway (eq 1,2,4) with a rate-determining protonation step (eq 1).[25] However, the positive shift of the catalytic wave relative to the Co(II)/Co(I) process suggests[25,25] that the first protonation is fast with respect to the following chemical steps. This consideration thus supports[25,25] the hypothesis that, under these experimental conditions, the hydrogen evolution catalysis by the **CoL0-4** complexes most likely proceeds via a heterolytic route (eq 3) rather than via a homolytic one (eq 4).‖

**Photocatalytic hydrogen evolution**

Photocatalytic hydrogen evolution experiments have been carried out for the class of **CoL0-4** catalysts upon continuous visible irradiation (175 W Xe arc lamp, cut-off filter at 400 nm) of argon-purged aqueous solutions (5 mL, 1 M acetate buffer at pH 5) containing 75 μM **CoL0-4** catalyst,¶ 0.5 mM Ru(bpy)₃Cl₂ as the photosensitizer, 0.1 M ascorbic acid as the

sacrificial electron donor and checking the gas-phase of the reactor by gas-chromatography. The choice of the pH was mainly dictated by comparison with photocatalytic systems involving the same sensitizer and sacrificial donor and already reported in the literature.[7a,11j,14] The kinetic traces (averages of three different experiments) are reported in Figure 2a, while related maximum turnover numbers (TONs) and frequencies (TOFs) are given in Figure 2b. In all cases hydrogen production levels off after approximately 2-3 hours of irradiation achieving maximum TONs between 56 and 94 with maximum TOFs between 2.1 and 3.3 min$^{-1}$ depending on the catalyst. A constant hydrogen production rate (where maximum TOFs have been calculated) is established after a short (few minutes) induction period. As previously observed on similar photochemical systems,[9f,11c,d,j,26] this can be related to the required lag-time to accumulate an appreciable fraction of doubly reduced, catalytically active species at steady state after that hydrogen evolution can take off.
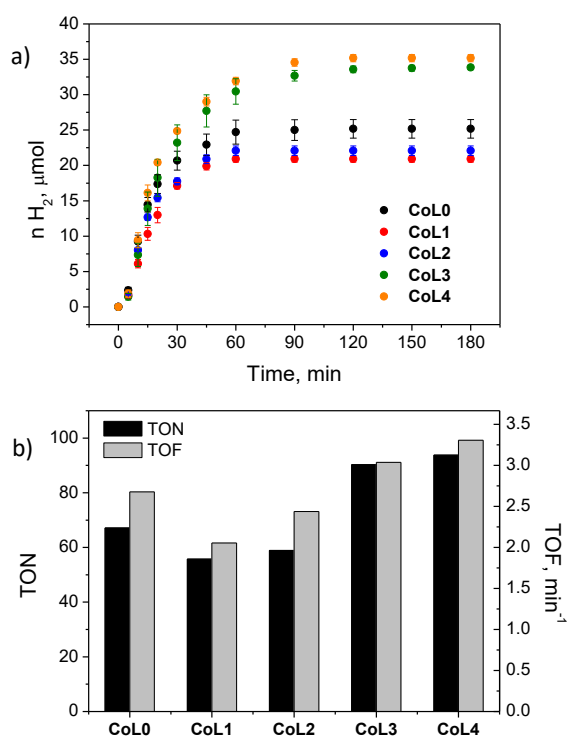


**Figure 2.** Photocatalytic hydrogen evolution experiments in 1 M acetate buffer solutions (5 mL, pH 5) containing 0.5 mM Ru(bpy)$_3$$^{2+}$, 0.1 M ascorbic acid and 75 μM **CoL0-4**: (a) hydrogen evolution kinetics (averages of three different experiments), (b) maximum turnover numbers and frequencies.

As far as the turnover limiting reactions are concerned, partial decomposition of both the photosensitizer and the catalyst can be deduced on the basis of the following considerations. Addition of the same amount of either the catalyst or the photosensitizer to a 1-hour photolyzed mixture (1 M acetate buffer at pH 5, 0.1 M ascorbic acid, 0.5 mM Ru(bpy)$_3$$^{2+}$, 75 μM **CoL0-4**) is such that the photocatalytic activity is only restored to an extent of ca 20-30% and ca 40-60%, respectively, in

terms of TON. On the other hand, more efficient hydrogen production is re-established when both the catalyst and the sensitizer are introduced after 1 hour photolysis with an overall recovery of up to 83% in terms of TON (Figure S5). The inability to thoroughly restore the same initial hydrogen evolving activity, in terms of both initial rate and maximum TON, is very likely attributable to accumulation in solution of decomposition products of the Ru(bpy)$_3$$^{2+}$ photosensitizer,[11c,14] competing in light absorption with the fresh sensitizer, and of the ascorbic acid sacrificial electron donor, namely dehydroascorbic acid, which is effective towards the short-circuiting quenching of transiently reduced species in solution (either of the sensitizer or of the catalyst).[11j,27]

In order to compare the photocatalytic activity of this class of cobalt complexes with related catalysts reported in the literature, it has to be considered that the hydrogen evolving performance is strictly dependent on the experimental conditions used, namely on the concentrations of the reactants, on the solvent medium, on the pH, and on the photon flux. Within these limitations, however, a qualitative comparison of the photochemical hydrogen evolving activity of the present systems with cobalt polypyridine complexes reported in the literature working in purely aqueous solutions in the presence of Ru(bpy)$_3$$^{2+}$ as the sensitizer and ascorbic acid as the sacrificial electron donor can be made.[11l] Such a comparison shows that **CoL0-4** catalysts perform similarly to the pentapyridine cobalt complexes reported by Long, Chang and coworkers[11a] as well as to the pentadentate cobalt catalyst described by Wang and coworkers[11h] and most of the pentacoordinated cobalt complexes reported by Crowley, Collomb, Blackman, and coworkers,[11k] but are less efficient than other polypyridine cobalt analogs such as the pentadentate complexes reported by Webster, Zhao, and coworkers,[14] the tetradentate catalysts by Castellano, Long, Chang, and coworkers,[11c] the quaterpyridine catalyst reported by Thummel and coworkers,[11g] the tetradentate complex reported by Ott and coworkers,[11f] and a pentapyridine cobalt complex recently reported by us.[11j]

**Photochemical mechanism for hydrogen evolution**

In homogeneous photocatalytic systems involving a hydrogen evolving catalyst (HEC), a photosensitizer (P), and a sacrificial electron donor (SD), the reduction of the catalyst to trigger hydrogen evolution may in principle occur by two different
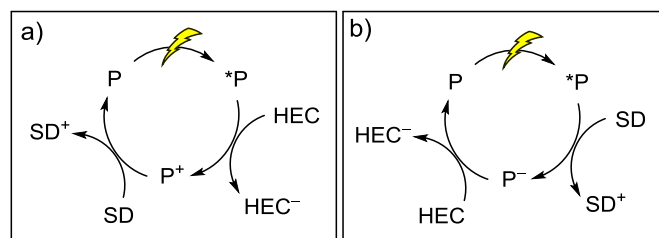


**Scheme 3.** Possible photochemical mechanisms for catalyst reduction in a homogeneous system for hydrogen production involving a catalyst (HEC), a photosensitizer (P), and a sacrificial electron donor (SD): (a) oxidative and (b) reductive pathways.

mechanisms:[9c,28] (i) an oxidative quenching pathway (Scheme 3a), involving first photoinduced electron transfer from the photosensitizer to the catalyst followed by hole shift to the sacrificial donor, or (ii) a reductive quenching pathway (Scheme 3b) whereby the excited sensitizer reacts first with the donor, yielding a photogenerated reductant which then undergoes a thermal electron transfer to the catalyst.

Basing on the first hypothesis (Scheme 3a), considering a redox potential of −1.12 V vs. SCE for the $Ru(bpy)_3^{3+}/^3*Ru(bpy)_3^{2+}$ couple[29] and the potentials for the Co(II)/Co(I) reduction (Figure 1a), oxidative quenching is thermodynamically unfavorable. On the other hand, reductive quenching of excited $Ru(bpy)_3^{2+}$ by ascorbic acid is allowed,[11,30] thus demonstrating the feasibility of a reductive mechanism (hypothesis ii, Scheme 3b). The bimolecular rate constant for this quenching process can be estimated by a classical Stern-Volmer analysis as $k = 2.1 \times 10^7$ $M^{-1}s^{-1}$ (Figure S6).

**Table 1.** Relevant photochemical data of the three-component system.

| Entry | $k_Q$ ($10^9$ $M^{-1}s^{-1}$) [a] | $k_{ET}$ ($10^9$ $M^{-1}s^{-1}$) [b] |
|---|---|---|
| CoL0 | 0.6 | 1.4 |
| CoL1 | 1.0 | 2.1 |
| CoL2 | 1.1 | 1.1 |
| CoL3 | 0.9 | 1.0 |
| CoL4 | 0.7 | 1.8 |

[a.] Bimolecular rate constants for quenching of the $Ru(bpy)_3^{2+}$ excited state obtained from photoluminescence data and the related Stern-Volmer analysis using a lifetime for the $Ru(bpy)_3^{2+}$ excited state decay of 400 ns; [b.] bimolecular rate constants for the electron transfer from the photogenerated $Ru(bpy)_3^+$ to the **CoL0-4** catalysts obtained by laser flash photolysis (excitation at 355 nm, analysis at 510 nm).

However, the luminescence of the $Ru(bpy)_3^{2+}$ photosensitizer is quenched by **CoL0-4** catalysts as well. From a Stern-Volmer treatment (Figure S7) it can be estimated that complexes **CoL0-4** quench the $Ru(bpy)_3^{2+}$ emission with bimolecular rate constants between $0.6\text{-}1.1 \times 10^9$ $M^{-1}s^{-1}$ (Table 1). Being oxidative quenching thermodynamically unfavorable, energy transfer to low lying cobalt *d-d* states[31] may very likely account for the observed photoreaction.

Under the experimental conditions used in the photocatalytic experiments, the ascorbic acid donor (0.1 M) is much more concentrated than the **CoL0-4** catalysts (75 μM). This translates into a higher pseudo-first order rate for the reductive quenching by the sacrificial donor ($2.1 \times 10^6$ $s^{-1}$) than for the catalyst quenching pathway ($4.5\text{-}8.3 \times 10^4$ $s^{-1}$). These results thus establish that the reductive quenching of triplet excited $Ru(bpy)_3^{2+}$ is the primary photochemical process within the donor/sensitizer/catalyst three-component systems examined and thus hydrogen evolution is triggered by a reductive photochemical pathway (Scheme 3b).

According to these considerations, one of the key processes which clearly deserves much attention is the electron transfer step from the photogenerated reducing sensitizer to the catalyst. Indeed, highly reducing species such as $Ru(bpy)_3^+$ are prone to decomposition in solution[32] and a fast electron scavenging is thus pivotal to minimize such an unproductive pathway. This electron transfer process can be conveniently

monitored by laser flash photolysis technique and time-resolved.[10h,11c,d,f,j,26,33] Upon excitation at 355 nm of a solution containing 0.1 mM $Ru(bpy)_3^{2+}$ and 0.1 M ascorbic acid in 1 M acetate buffer at pH 5, the evolution of the $Ru(bpy)_3^{2+}$ triplet excited manifold to yield the reduced $Ru(bpy)_3^+$ species via reductive quenching by ascorbic acid is observed (Figure 3a).

This process is accompanied by the decrease of the absorption at 380 nm and of the MLCT bleach centered at 450 nm (typical of the $^3*Ru(bpy)_3^{2+}$) and the development of a transient absorption at 510 nm, which is characteristic of the reduced $Ru(bpy)_3^+$ species.[11c,d,f,j,26,33,34] This signal then decays to the baseline in a time-scale of hundred μs by bimolecular recombination with the oxidized ascorbate radical (Figure 3b).[11d,33]
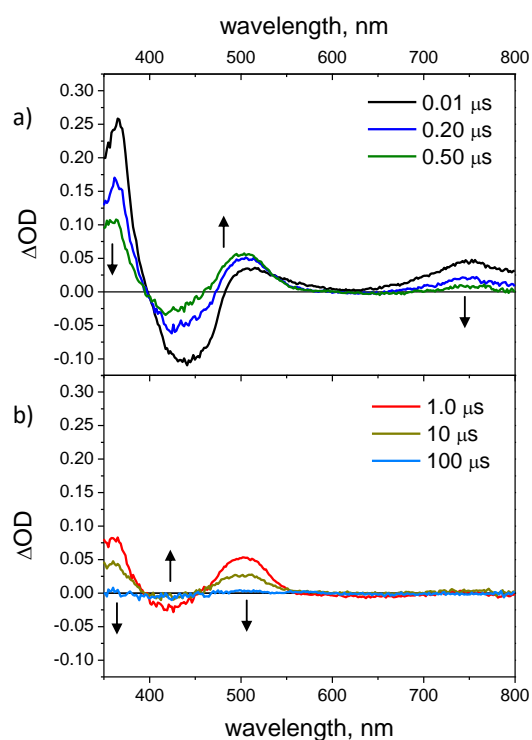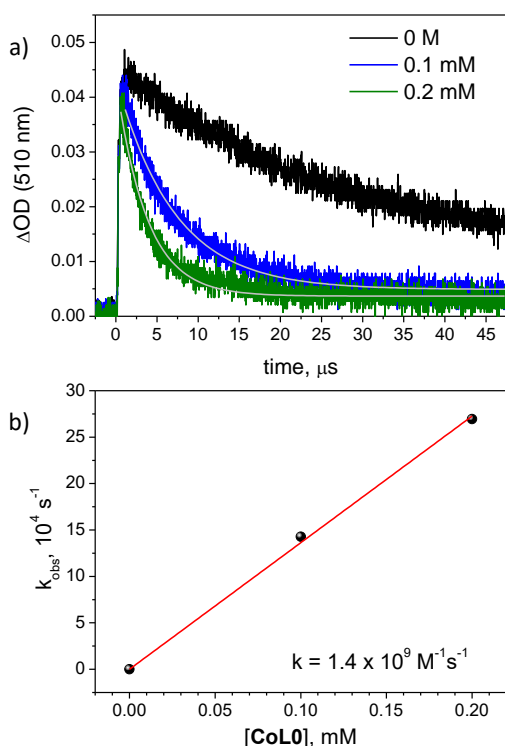


**Figure 3.** Transient absorption spectra obtained by laser flash photolysis (excitation at 355 nm) of a 1 M acetate buffer (pH 5) solution containing 100 μM $Ru(bpy)_3^{2+}$ and 0.1 M ascorbic acid at (a) 0.01-0.50 μs and (b) 1-100 μs time delays.

A similar sequence of photochemical events is also observed when **CoL0-4** catalysts are introduced in the same reaction mixtures (formation of the reduced $Ru(bpy)_3^+$ species via bimolecular reductive quenching by the ascorbic acid donor), differing essentially for a much faster disappearance of the 510-nm absorption. This faster decay can be reasonably assigned to the electron transfer process occurring from the photogenerated $Ru(bpy)_3^+$ to the catalyst. Moreover, this transient absorption decays with an appreciable first-order dependence on catalyst concentration and under pseudo-first order kinetic conditions (i.e., [**CoL0-4**] >> [$Ru(bpy)_3^+$]) a bimolecular rate constant can be obtained for such an electron transfer process (Figure 4 for **CoL0** and Figure S8 for the remaining **CoL1-4** catalysts, data are reported in Table 1). These estimates yield values in the range $1.0\text{-}2.1 \times 10^9$ $M^{-1}s^{-1}$,

close to the diffusion limit and within the same order of magnitude of the bimolecular electron transfer rates from Ru(bpy)$_3^+$ to other polypyridine cobalt complexes,[11c,d,f,j] to a tetracationic cobalt porphyrin,[26] and to a cobaloxime.[33]

These values are quite similar throughout the **CoL0-4** series, as expected on the basis of the similar redox potentials and thus on the resulting driving forces for the electron transfer processes. Importantly, analysis of the decay of the Ru(bpy)$_3^+$ species at different wavelengths (taking **CoL0** as a representative case for all catalysts, Figure S9) show no appreciable formation and accumulation of additional transient signals, e.g. those expected for the generation of a Co(I) moiety, which is supposed to display featuring absorption signatures in the visible spectrum between 500-700 nm.[11c,f]



**Figure 4.** (a) Kinetic traces at 510 nm obtained by laser flash photolysis (excitation at 355 nm) of a 1 M acetate buffer (pH 5) solution containing 100 µM Ru(bpy)$_3^{2+}$, 0.1 M ascorbic acid, 0-0.2 mM **CoL0**; (b) plot of the observed rate (obtained from a single-exponential fitting of the kinetic traces) vs. **CoL0** concentration for the estimation of the bimolecular rate constant.

This suggests that herein the electron transfer from the photogenerated Ru(bpy)$_3^+$ species most likely occurs together with a protonation step as a concerted proton-coupled electron-transfer process (see above eq 1), whose product, namely the Co(III)-H species, is known to lack any appreciable absorption above 500 nm.[35]

**Effect of the substituent on hydrogen evolution**

The approach adopted herein to tune the catalytic activity by the tetradentate cobalt complex was motivated by the idea that the different substituents at the phenyl ring, having different hydrogen bonding donor or acceptor abilities,[36] were

expected to display different molecular interactions with the solvent environment, i.e. with the surrounding water molecules. In other words, the substituents were expected to assist the proton coupled electron transfer (PCET) processes required to foster hydrogen evolution (i.e. the formation of the cobalt(III)-hydride intermediate and the protonation of the cobalt(II)-hydride species). A comparison of the photochemical hydrogen evolution performances among the **CoL0-4** complexes shows that some differences do actually exist with maximum TONs between 56 and 94 and maximum TOFs between 2.1 and 3.3 min$^{-1}$ (Figure 2).

On a TON basis, the highest values are obtained for complexes **CoL3** and **CoL4** (90 and 94, respectively), while lower TONs are detected for the remaining catalysts in the order **CoL0** > **CoL2** > **CoL1** (67, 59, and 56, respectively). Therefore, the presence of different substituents on the phenylpyridine moiety plays an important role in the stabilization of the catalytic unit. Although the degradation routes involving the cobalt catalyst are actually unknown, it can be argued that the presence of potentially reducible functional groups such as the aldehyde and the amide might offer alternative reaction pathways to the cobalt hydride intermediates. Accordingly, the involvement of the ligand framework in the reaction can thus result into an enhanced decomposition of the catalytic unit.

When the comparison is made in terms of maximum TOFs (which can be intrinsically related to the quantum yield of hydrogen evolution, being calculated in the linear part of the kinetic traces), it can be observed that larger values are measured in the case of complexes **CoL3**, and **CoL4** (3.0, and 3.3 min$^{-1}$, respectively), while lower values are measured in the order for **CoL0**, **CoL2**, and **CoL1** (2.7, 2.4, and 2.1 min$^{-1}$, respectively). Since the primary photochemical step, namely the photogeneration of the Ru(bpy)$_3^+$ reducing agent, is independent of the **CoL0-4** catalyst used, possible reasons accounting for the observed evidences must rely on the dark catalytic process. Differences in terms of electron transfer rates (eq 1,2) can be clearly ruled out since the rates of catalyst activation (eq 1) by the photogenerated reduced sensitizer are generally high and comparable along the **CoL0-4** series (Table 1) and a similar trend can be also expected for the second electron transfer reaction (eq 2). Accordingly, differences must be found on the chemical protonation step. On a tentative basis it can be envisaged that the hanging groups can be involved in hydrogen bonding with water and may consequently favor the formation of a network of solvent molecules in proximity of the cobalt center, thus speeding up the protonation step required in the HER mechanism (eq 3) and therefore catalysis. The good hydrogen-bonding abilities (both as donor and acceptor) of the hydroxo groups[36] are indeed consistent with this hypothesis. It must be remarked, however, that the observed differences in terms of maximum TOFs are not that large among the **CoL0-4** series, pointing out that the actual effect on the kinetics played by the dangling substituents is indeed intrinsically small. This observation can be rationalized considering the weak electronic effects exerted by the dangling substituents on the Co(II)/Co(I) reduction potential (see above), which strongly suggests that the phenyl

ring is electronically decoupled from the pyridine, with substantially wide dihedral angles. Under these assumptions, the dangling functional groups should be in fact located far apart with respect to the cobalt center, thus being only marginally effective in promoting and assisting the formation of the relevant catalytic intermediates.

## Conclusions

A series of new cobalt polypyridine catalysts (**CoL0-4**), based on the tetradentate **TPMA** ligand bearing different functional groups, has been synthesized and studied as hydrogen evolving catalysts in light-assisted conditions in the presence of the standard $Ru(bpy)_3^{2+}$/ascorbic acid sensitizer/donor couple. Upon continuous visible irradiation of the three-component catalyst/sensitizer/donor system, hydrogen is produced with TONs between 56 and 94, maximum TOFs between 2.1 and 3.3 $min^{-1}$. In all these cases the photocatalytic activity is mainly limited by decomposition of both the sensitizer and the catalyst. The mechanism towards hydrogen evolution is triggered by bimolecular reductive quenching of the $Ru(bpy)_3^{2+}$ photosensitizer by the ascorbic acid donor, followed by bimolecular electron transfer to the catalyst, taking place at remarkable rates close to the diffusion limit. The enhanced activity by **CoL3** and **CoL4** with respect to the remaining complexes is attributable, on a TON basis, to the enhanced stability under photocatalytic conditions arising from the absence of potentially reactive functional groups as in the case of **CoL1** and **CoL2**, and, on a TOF basis, to faster catalysis rates. As to the latter point, the presence of good hydrogen-bonding substituents, such as the hydroxo group, may indeed favor the formation of a water network near the cobalt center thus accelerating the protonation step required in the HER mechanism. Although this effect is present, the substantially small differences observed within the **CoL0-4** series demonstrate that the tuning approach adopted herein is not that effective, which can be ascribed to the non-optimal structural arrangement featuring large distances between the dangling functional group and the cobalt center. Accordingly, the modification of the ligand pool to increase the rigidity of the phenylpyridine moiety can be a viable solution to enhance the envisaged second-sphere effect on the HER catalysis. Research towards this direction is currently planned in our laboratories.

## Acknowledgements

## Experimental Section

**Materials.** Chemicals were purchased from Sigma Aldrich and TCI chemicals and used without further purification. Acetonitrile for electrochemistry was of electrochemical grade. Milli-Q ultrapure water and related buffers were used for the electrochemical, spectroscopic, and photocatalytic experiments.

**NMR.** $^1H$ and $^{13}C\{1H\}$ NMR spectra were recorded at 301 K on a Bruker AC-400, AC-300, and AC-200 MHz instruments. The $^1H$ NMR spectra were referenced to the solvent residual peak of MeOD-$d_4$ (3.31 ppm) or $CD_3CN$-$d_3$ (1.94 ppm); the $^{13}C$ NMR spectra (50 MHz) were referenced to MeOD ($49.00\pm0.02$ ppm) or $CD_3CN$ peaks ($1.32\pm0.02$ and $118.26\pm0.02$ ppm).

**ESI-MS.** ESI-MS experiments were carried out in positive mode with an Agilent Technologies LC/MSD Trap SL AGILENT instrument (mobile phase methanol or acetonitrile). MS peaks are reported as monoisotopic mass. Microanalyses were performed with a Flash 2000 Thermo Scientific Analyser.

**Electrochemistry.** Cyclic Voltammetry (CV) measurements were carried out with a PC-interfaced *Eco Chemie Autolab/Pgstat 30* Potentiostat. A conventional three-electrode cell assembly was adopted: a saturated calomel electrode (SCE Amel) and a platinum electrode, with the former separated from test solution by a glass frit, were used as reference and counter electrodes, respectively; a glassy carbon (GC) electrode (7 $mm^2$ surface area) was used as the working electrode. All experiments were performed in nitrogen-purged solutions and the working electrode was accurately polished with alumina slurry after every single scan. Potential controlled electrolysis experiments were performed in a gas-tight custom-made electrochemical cell using a carbon foil (1 $cm^2$ surface area, 0.5 mm thickness) as the working electrode, a platinum wire as the counter electrode (separated from the test solution by a frit) and a Ag/AgCl (3 M NaCl) as the reference electrode (in the text, potentials are converted to SCE for uniformity with CV experiments). The head-space of the cell was connected to the gas-chromatography (GC) apparatus (see below for details) for the determination and quantification of hydrogen. The calibration was performed through a galvanostatic electrolysis of a 0.1 M $H_2SO_4$ solution at 2 mA current, using a platinum wire as the working electrode, assuming 100% Faradaic yield towards hydrogen formation.

**Optical spectroscopy.** UV-Vis absorption spectra were recorded on a *Jasco V-570 UV/Vis/NIR* spectrophotometer. Emission spectra were taken on a *Horiba-Jobin Yvon Fluoromax-2* spectrofluorimeter, equipped with a *Hamamatsu R3896* tube. Nanosecond transient measurements were performed with a custom laser spectrometer comprised of a *Continuum Surelite II* Nd:YAG laser (FWHM 6-8 ns) with frequency doubled, (532 nm, 330 mJ) or tripled, (355 nm, 160 mJ) option, an *Applied Photophysics* xenon light source including a mod. 720 150 W lamp housing, a mod. 620 power controlled lamp supply and a mod. 03-102 arc lamp pulser. Laser excitation was provided at 90° with respect to the white light probe beam. Light transmitted by the sample was focused

onto the entrance slit of a 300 mm focal length *Acton SpectraPro 2300i* triple grating, flat field, double exit monochromator equipped with a photomultiplier detector (*Hamamatsu R3896*) and a *Princeton Instruments PIMAX II* gated intensified CCD camera, using a *RB Gen II* intensifier, a ST133 controller and a PTG pulser. Signals from the photomultiplier (kinetic traces) were processed by means of a *LeCroy 9360* (600 MHz, 5 Gs/s) digital oscilloscope.

**Hydrogen evolution experiments.** The hydrogen evolution experiments were carried out upon continuous visible light irradiation with a 175 W xenon arc-lamp (*CERMAX PE175BFA*) of a reactor containing the solution (a 10 mm pathlength pyrex glass cuvette with head space obtained from a round-bottom flask). A cut-off filter at 400 nm and a hot mirror (IR filtering) have been used to provide the useful wavelength range (400-800 nm). The reactor is placed at a distance of 20 cm from the irradiation source and the light beam is completely focused on the reactor (all the solution is irradiated during the experiment). The measuring cell is sealed during the photoreaction: the head to which cell is attached has indeed four ports, closed with Swagelok® connections, two of them are part of a closed loop involving GC gas inlet and sample vent in order to analyze head space content without an appreciable gas consumption, and the other two are for the degassing procedure (input and output). The gas phase of the reaction vessel was analyzed on an *Agilent Technologies 490 microGC* equipped with a 5 Å molecular sieve column (10 m), a thermal conductivity detector, and using Ar as carrier gas. 5 mL from the headspace of the reactor are sampled by the internal GC pump and 200 nL are injected in the column maintained at 60°C for separation and detection of gases. The unused gas sample is then reintroduced in the reactor in order to minimize its consumption along the whole photolysis. The amount of hydrogen was quantified through the external calibration method. This procedure was performed, prior to analysis, through a galvanostatic (typically 1 mA) electrolysis of a 0.1 M $H_2SO_4$ solution in an analogous cell (same volume) equipped with two Pt wires sealed in the glass at the bottom of the cell. A 100% faradaic efficiency was assumed leading to a linear correlation between the amount of $H_2$ evolved at the cathode and the electrolysis time. In a typical experiment, samples of 5 mL were prepared in 20 mL scintillation vials starting from a 1 M acetate buffer (pH 5) solution of $Ru(bpy)_3Cl_2$ (0.5 mM), and further adding ascorbic acid (as solid) and the **CoL0-4** catalyst (small aliquots from a concentrated mother solution in acetonitrile). The change in volume upon addition of the latter can be always considered negligible (dilution $\leq$ 1%). The solution was then put in the reactor, degassed by bubbling Ar for 30 min, and thermostated at 15°C. The cell was then irradiated and the solution continually stirred during the photolysis. The gas phase of the reaction was analyzed through GC and the amount of hydrogen quantified.

## Notes and references

‡ With respect to standard electrocatalytic studies usually performed in neat acetonitrile, herein we introduced water into the reaction medium to evaluate the effect on electrocatalysis by the different substituents since the interaction of protons with the functional groups can be only mediated by water (i.e., via hydrogen bonding). To this aim we took advantage of a 50/50 acetonitrile/water mixture, chosen for comparison with literature studies on related cobalt complexes.[15a]

§ A hint of catalytic wave can be indeed detected at potentials compatible with the Co(II)/Co(I) process.

§§ This is also consistent with the fact that, with the exception of **CoL1** for which some decomposition is likely to occur particularly at higher TFA concentration), comparable slopes (between 0.032 and 0.028 $A\cdot M^{-1}$, Figure S3) are observed in the linear correlation between the catalytic peak current and [TFA].

∥ It should be emphasized that the ECEC mechanism (eq 1,2,3) for hydrogen evolution by the **CoL0-4** complexes is only a proposed catalytic pathway according to the available experimental data. For a more conclusive account additional experimental conditions should be indeed tested and further analyses performed, including full determination of kinetic constants. This is, however, out of the scope of this manuscript.

¶ Under the conditions explored, hydrogen evolving activity was detectable in the presence of **CoL0-5** catalysts at concentrations ≥10 μM. However, in order to evaluate the different photocatalytic performances within the class of **CoL0-4** complexes a catalyst concentration of 75 μM has been chosen providing substantial hydrogen production for an accurate comparison.

1   (a) J. H. Alstrum-Acevedo, M. K. Brennaman and T. J. Meyer, *Inorg. Chem.* 2005, **44**, 6802. (b) N. S. Lewis and D. G. Nocera, *Proc. Natl. Acad. Sci. U.S.A.* 2006, **103**, 15729. (c) R. Eisenberg and H. B. Gray, *Inorg. Chem.* 2008, **47**, 1697. (d) D. G. Nocera, *Inorg. Chem.* 2009, **48**, 10001. (e) H. B. Gray, *Nat. Chem.* 2009, **1**, 7. (f) N. Armaroli, V. Balzani and N. Serpone, *Powering Planet Earth: Energy Solutions for the Future*, Wiley, New York, 2012. (g) D. Gust, T. A. Moore and A. L. Moore, *Faraday Disc.* 2012, **155**, 9. (h) J. R. McKone, N. S. Lewis and H. B. Gray, *Chem. Mater.* 2014, **26**, 407. (i) M. Natali and F. Scandola. *Supramolecular Artificial Photosynthesis*. G. Bergamini, S. Silvi (eds.), *Applied Photochemistry*, *Lecture Notes in Chemistry* **92**, DOI: 10.1007/978-3-319-31671-0_1, Springer 2016.

2   J. R. McKone, S. C. Marinescu, B. S. Brunschwig, J. R. Winkler and H. B. Gray, *Chem. Sci.* 2014, **5**, 865.

3   (a) J. Kiwi and M. Grätzel, *Nature* 1979, **281**, 657. (b) J.-M. Lehn and J.-P. Sauvage, *Nouv. J. Chim.* 1977, **1**, 449. (c) A. J. Bard and M. A. Fox, *Acc. Chem. Res.* 1995, **28**, 141.

4   S. Y. Reece, J. A. Amel, K. Sung, T. D. Jarvi, A. J. Esswein, J. J. H. Pijpers and D. G. Nocera, *Science* 2011, **334**, 645.

5   (a) D. Merki, H. Vrubel, L. Rovelli, S. Fierro and X. Hu, *Chem. Sci.* 2012, **3**, 2515. (b) P. D. Tran, M. Nguyen, S. S. Pramana, A. Bhattacharjee, S. Y. Chiam, J. Fize, M. J. Field, V. Artero, L. H. Wong, J. Loo and J. Barber, *Energy Environ. Sci.* 2012, **5**, 8912.

6   (a) D. G. Nocera, *Acc. Chem. Res.* 2012, **45**, 767; (b) J. P. Torella, C. J. Gagliardi, J. S. Chen, D. K. Bediako, B. Colon, J. C. Way, P. A. Silver and D. G. Nocera, *Proc. Natl. Acad. Sci. U.S.A.* 2015, **112**, 2337.

7   (a) D. Streich, Y. Astuti, M. Orlandi, L. Schwartz, R. Lomoth, L. Hammarström and S. Ott, *Chem. Eur. J.* 2010, **16**, 60; (b) S. Pullen, H. Fei, A. Orthaber, S. Cohen and S. Ott, *J. Am. Chem. Soc.* 2013, **135**, 16997.

8   (a) M. L. Helm, M. P. Stewart, R. M. Bullock, M. Rakowski DuBois and D. L. DuBois, *Science* 2011, **333**, 863. (b) M. P. McLaughlin, T. M. McCormick, R. Eisenberg and P. L. Holland, *Chem. Commun.* 2011, **47**, 7989. (c) M. A. Gross, A. Reynal, J. Durrant and E. Reisner, *J. Am. Chem. Soc.* 2014, **136**, 356. (d) A. S. Weingarten, R. V. Kazantsev, L. C. Palmer, M.

McClendon, A. R. Koltonow, A. P. S. Samuel, D. J. Kiebala, M. R. Wasielewski and S. I. Stupp, *Nat. Chem.* 2014, **6**, 964.

9   (a) S. Losse, J. G. Vos and S. Rau, *Coord. Chem. Rev.* 2010, **254**, 2492. (b) V. Artero, M. Chavarot-Kerlidou and M. Fontecave, *Angew. Chem., Int. Ed.* 2011, **50**, 7238. (c) W. T. Eckenhoff, W. R. McNamara, P. Du and R. Eisenberg, *Biochim. Biophys. Acta* 2013, **1827**, 958. (d) C. C. L. McCrory, C. Uyeda and J. C. Peters, *J. Am. Chem. Soc.* 2012, **134**, 3164. (e) S. Varma, C. E. Castillo, T. Stoll, J. Fortage, A. G. Blackman, F. Molton, A. Deronzier and M.-N. Collomb, *Phys. Chem. Chem. Phys.* 2013, **15**, 17544. (f) C. Gimbert-Suriñach, J. Albero, T. Stoll, J. Fortage, M.-N. Collomb, A. Deronzier, E. Palomares and A. Llobet, *J. Am. Chem. Soc.* 2014, **136**, 7655. (g) R. Gueret, C. E. Castillo, M. Rebarz, F. Thomas, A.-A. Hargrove, J. Pécaut, M. Sliwa, J. Fortage and M.-N. Collomb, *J. Photochem. Photobiol. B* 2015, **152**, 82. (h) S. Roy, M. Bacchi, G. Berggren and V. Artero, *ChemSusChem* 2015, **8**, 3632.

10  (a) P. Du, K. Knowles and R. Eisenberg, *J. Am. Chem. Soc.* 2008, **130**, 12576. (b) A. Fihri, V. Artero, M. Razavet, C. Baffert, W. Leibl and M. Fontecave, *Angew. Chem., Int. Ed.* 2008, **47**, 564. (c) T. M. McCormick, B. D. Calitree, A. Orchard, N. D. Kraut, F. V. Bright, M. R. Detty and R. Eisenberg, *J. Am. Chem. Soc.* 2010, **132**, 15480. (d) J. L. Dempsey, J. R. Winkler and H. B. Gray, *J. Am. Chem. Soc.* 2010, **132**, 1060. (g) F. Lakadamyali, A. Reynal, M. Kato, J. R. Durrant and E. Reisner, *Chem. Eur. J.* 2012, **18**, 15464. (h) M. Natali, R. Argazzi, C. Chiorboli, E. Iengo and F. Scandola, *Chem. Eur. J.* 2013, **19**, 9261. (i) M. Natali, M. Orlandi, C. Chiorboli, E. Iengo, V. Bertolasi and F. Scandola, *Photochem. Photobio. Sci.* 2013, **12**, 1749. (j) K. Peuntinger, T. Lazarides, D. Dafnomili, G. Charalambidis, G. Landrou, A. Kahnt, R. P. Sabatini, D. W. McCamant, D. T. Gryko, A. G. Coutsolelos and D. M. Guldi, *J. Phys. Chem. C* 2013, **117**, 1647.

11  (a) Y. Sun, J. Sun, J. R. Long, P. Yang and C. J. Chang, *Chem. Sci.* 2013, **4**, 118. (b) M. Nippe, R. S. Khnayzer, J. A. Panetier, D. Z. Zee, B. S. Olaiya, M. Head-Gordon, C. J. Chang, F. N. Castellano and J. R. Long, *Chem. Sci.* 2013, **4**, 3934. (c) R. S. Khnayzer, V. A. Thoi, M. Nippe, A. E. King, J. W. Jurss, K. A. El Roz, J. R. Long, C. J. Chang and F. N. Castellano, *Energy Environ. Sci.* 2014, **7**, 1477. (d) B. Shan, T. Baine, X. A. N. Ma, X. Zhao and R. H. Schmehl, *Inorg. Chem.* 2013, **52**, 4853. (e) C. Bachmann, M. Guttentag, B. Spingler and R. Alberto, *Inorg. Chem.* 2013, **52**, 6055. (f) W. M. Singh, M. Mirmohades, R. T. Jane, T. A. White, L. Hammarström, A. Thapper, R. Lomoth and S. Ott, *Chem. Commun.* 2013, **49**, 8638. (g) L. Tong, R. Zong and R. P. Thummel, *J. Am. Chem. Soc.* 2014, **136**, 4881. (h) J. Xie, Q. Zhou, C. Li, W. Wang, Y. Hou, B. Zhang and X. Wang, *Chem. Commun.* 2014, **50**, 6520. (i) C.-F. Leung, S.-M. Ng, C.-C. Ko, W.-L. Man, J. Wu, L. Chen and T.-C. Lau, *Energy Environ. Sci.* 2012, **5**, 7903. (j) E. Deponti, A. Luisa, M. Natali, E. Iengo and F. Scandola, *Dalton Trans.* 2014, **43**, 16345. (k) W. K. C. Lo, C. E. Castillo, R. Gueret, J. Fortage, M. Rebarz, M. Sliwa, F. Thomas, C. J. McAdam, G. B. Jameson, D. A. McMorran, J. D. Crowley, M.-N. Collomb and A. G. Blackman, *Inorg. Chem.* 2016, **55**, 4564. (l) N. Queyriaux, R. T. Jane, J. Massin, V. Artero and M. Chavarot-Kerlidou, *Coord. Chem. Rev.* 2015, **304-305**, 3.

12  A. Call, Z. Codolá, F. Acuña-Pares and J. Lloret-Fillol, *Chem. Eur. J.* 2014, **20**, 6171.

13  (a) D. W. Wakerley and E. Reisner, *Phys. Chem. Chem. Phys.* 2014, **16**, 5739. (b) A. Panagiotopoulos, K. Ladomenou, D. Sun, V. Artero and A. G. Coutsolelos, *Dalton Trans.* 2016, **45**, 6732.

14  M. Vennampalli, G. Liang, L. Katta, C. E. Webster and X. Zhao, *Inorg. Chem.* 2014, **53**, 10094.

15  (a) W. R. McNamara, Z. Han, P. J. Alperin, W. W. Brennessel, P. L. Holland and R. Eisenberg, *J. Am. Chem. Soc.* 2011, **133**, 15368. (b) W. R. McNamara, Z. Han, C.-J. Yin, W. W. Brennessel, P. L. Holland and R. Eisenberg, *Proc. Natl. Acad. Sci. U.S.A.* 2012, **109**, 15594.

16  A. Mahammed, B. Mondal, A. Rana, A. Dey and Z. Gross, *Chem. Commun.* 2014, **50**, 2725.

17  C. H. Lee, D. K. Dogutan and D. G. Nocera, *J. Am. Chem. Soc.* 2011, **133**, 8775.

18  (a) F. A. Scaramuzzo, G. Licini and C. Zonta, *Chem. Eur. J.* 2013, **19**, 16809. (b) E. Badetti, K. Wurst, G. Licini and C. Zonta, *Chem. Eur. J.* 2016, **22**, 6515. (c) R. Berardozzi, E. Badetti, N. A. Carmo dos Santos, K. Wurst, G. Licini, G. Pescitelli and C. Zonta, *Chem. Commun.* 2016, **52**, 8428.

19  J. T. Muckerman and E. Fujita, *Chem. Commun.* 2011, **47**, 12456.

20  J. L. Dempsey, B. S. Brunschwig, J. R. Winkler and H. B. Gray, *Acc. Chem. Res.* 2009, **42**, 1995.

21  A. J. Bard and L. R. Faulkner, *Electrochemical Methods: Fundamentals and Applications*, 2nd ed.; John Wiley and Sons: New York, 2001.

22  J. P. Bigi, T. E. Hanna, W. H. Harman, A. Chang and C. J. Chang, *Chem. Commun.* 2010, **46**, 958.

23  (a) J.-M. Savéant and K. B. Su, *J. Electroanal. Chem.* 1984, **171**, 341. (b) J.-M. Savéant, *Chem. Rev.* 2008, **108**, 2348.

24  E. S. Rountree, D. J. Martin, B. D. McCarthy and J. L. Dempsey, *ACS Catalysis* 2016, **6**, 3326.

25  (a) C. Costentin and J.-M. Savéant, *ChemElectroChem* 2014, **1**, 1226. (b) C. Costentin, H. Dridi and J.-M. Savéant, *J. Am. Chem. Soc.* 2014, **136**, 13727.

26  M. Natali, A. Luisa, E. Iengo and F. Scandola, *Chem. Commun.* 2014, **50**, 1842.

27  C. Bachmann, B. Probst, M. Guttentag and R. Alberto, *Chem. Commun.* 2014, **50**, 6737.

28  (a) E. S. Andreiadis, M. Chavarot-Kerlidou, M. Fontecave and V. Artero, *Photochem. Photobio.* 2011, **87**, 946; (b) K. Ladomenou, M. Natali, E. Iengo, G. Charalampidis, F. Scandola and A. G. Coutsolelos, *Coord. Chem. Rev.* 2015, **304-305**, 38.

29  A. Juris, V. Balzani, F. Barigelletti, S. Campagna, P. Belser and A. Von Zelewsky, *Coord. Chem. Rev.* 1988, **84**, 85.

30  G. M. Brown, B. S. Brunschwig, C. Creutz, J. F. Endicott and N. Sutin, *J. Am. Chem. Soc.* 1979, **101**, 1298.

31  B. Probst, M. Guttentag, A. Rodenberg, P. Hamm and R. Alberto, *Inorg. Chem.* 2011, **50**, 3403.

32  C. V. Krishnan and N. Sutin, *J. Am. Chem. Soc.* 1981, **103**, 2141.

33  E. Deponti and M. Natali, *Dalton Trans.* 2016, **45**, 9136.

34  L. A. Kelly and M. A. J. Rodgers, *J. Phys. Chem.* 1994, **98**, 6377.

35  (a) C. Creutz, H. A. Schwarz, J. F. Wishart, E. Fujita and N. Sutin, *J. Am. Chem. Soc.* 1991, **113**, 3361. (b) A. Lewandowska-Andralojc, T. Baine, X. Zhao, J. T. Muckermann, E. Fujita and D. E. Polyansky, *Inorg. Chem.* 2015, **54**, 4310.

36  P. Gilli, L. Pretto, V. Bertolasi and G. Gilli, *Acc. Chem. Res.* 2009, **42**, 33.